



Eigenfrequency analysis of the vibrating horn in Ultrasonic Metal Welding

Elie Abi Raad, Jose Maria Uribe, Michael Vorländer

Institute for Hearing Technology and Acoustics
RWTH Aachen University
ear@akustik.rwth-aachen.de

Abstract

Ultrasonic Metal Welding is a friction welding process that relies on transmitting horizontal vibrations from a piezoelectric transducer to the workpieces that should be welded. The last part of this transmission chain, and the main component that transmits vibrations to the workpieces, is the horn. Although widely used, ultrasonic metal welding still suffers from fluctuations in the strength of the weld that it produces. In addition, and though the welding frequency is mainly around 20 kHz, measurements of the vibrations of the horn during welding show nonlinear vibrations with additional spectral components in the whole measurement range, up to 120 kHz. These extra vibrations might be a source of problems during welding as well as a source of information. Therefore, a better understanding of the vibrational field in the horn is needed. In this work, the eigenmodes of the horn are simulated and analysed, and potentially problematic modes of vibration are identified.

Keywords: Ultrasonic Metal Welding, modal analysis, vibroacoustics, simulations

1 Introduction

Ultrasonic Metal Welding (USMW) is a type of friction welding that is often used for electronics, for example in welding battery tabs [1]. Despite its wide industrial use, the strength of the welds produced in USMW still fluctuates from weld to weld, and finding the right welding parameters for a specific welding configuration can take time and trial and error. The exact causes of the strength fluctuations are still unknown, as there are many parameters which can affect the weld formation. Even the exact way the weld formation takes place is still a subject of study, with new theories being proposed as recently as 2020 [1].

Put simply, USMW happens in the following way: the workpieces, the metal sheet which are meant to be welded, are placed on top of each other on a machine component called *anvil*. Then, another component of the machine, called *horn* or *sonotrode*, compresses the workpieces against each other and against the anvil by applying a downward vertical force on them. A transducer then generates horizontal vibrations, which are transmitted to the horn via a component called “booster”. The horn then starts to vibrate sinusoidally along the horizontal direction at a frequency around 20 kHz and a displacement amplitude of about 20 μm . In doing so, the horn, top worksheet, bottom worksheet and anvil move relative to each other, creating friction at the interfaces, and ultimately leading to the formation of a weld between the top sheet and bottom sheet [1][2].

In reality, the actual vibrations of the horn are more complex. Measurements [3][4] have shown that, during welding, the horn vibrates at many frequencies other than the welding frequency. These frequencies include harmonics of the welding frequency, but also other frequencies as well. It is assumed that the additional frequencies are created in a nonlinear process in the excitation by the transducer. Such frequencies of vibrations were measured by the authors at the welding tip of the horn, a few centimeters above the interface between the

top workpiece and the horn as seen in Figure 1, and include frequencies both higher and lower than the welding frequency. The experimental data and the experimental procedure were already presented in [3], but only part of the results were presented in those papers.

As the horn is excited at multiple frequencies, it is possible that some of those frequencies significantly excite eigenmodes of the horn. It is possible that some of those eigenmodes include a notable displacement of the welding tip of the horn in the vertical direction, into and away from the workpieces, which might affect the force applied by the horn on the workpieces. USMW, as its categorisation as a friction welding process suggests, relies heavily on the friction between the horn, the workpieces and the anvil. Friction itself depends heavily on the force applied by the horn on the workpieces, as well as the relative displacements between them. Therefore, the welding process might be affected by these extra frequencies, and better knowledge of the movement of the welding tip of the horn during welding is needed. Some displacement of the horn into the workpieces is already an integral part of USMW, with typical penetration depths starting at around 100 μm and increasing with welding time [5].

The goal of this paper is to offer insight into USMW by studying the vibrations of the horn, the machine component directly responsible for welding. In this study, a modal analysis of the horn vibrations via simulations is done. The eigenfrequencies of the horn are derived and compared to experimental measurements. Since a very important factor for the formation of a weld in USMW is friction, and friction depends directly on the vertical force applied by the horn on the workpieces, the eigenmodes are investigated as well to see whether they might affect the force applied by the horn on the workpieces. One should note two elements: first, the horn is modelled as a LTI system in this study. Second, this study was done for a single horn geometry. In USMW, horn geometries are highly variable, and are often customised to the type of weld required. Therefore, the results shown in this study should not be generalised blindly to any horn geometry, but should rather be taken as a case example, and the results should be extended to multiple horn geometries.

2 Measurements and simulations

2.1 Experimental data acquisition

The experimental data and the experimental procedure were already presented in [3], but only part of the results were presented in those papers. A short recapitulation of the measurement procedure will be given here. For more information on the welding parameters, the reader is invited to refer to [3].



Figure 1: Measurement point on the horn, in the white circle (repeated from [3])

The vibrations of the horn were measured during welding along the direction of welding using a Polytec CLV-2534 laser Doppler vibrometer, which measured the velocity of the horn. The velocity was later integrated to get the displacement vibrations. The measurement point was taken a few centimetres above the top sheet-horn interface, as shown in Figure 1. The workpieces welded were CW-008A copper sheets, of dimensions 125 mm x 45 mm x 0.5 mm (length x width x thickness), welded along the width. The amplitude of vibration of the horn at the welding frequency was 25 μm . The sampling rate of the measurement system was 250 kHz, and the vibrations were measured up to 125 kHz.

The direction of measurement is important to note, because no vibrations in other directions were measured. This means that no information about the vibrations of the horn in any other direction, for example vertically, is available.

2.2 Simulation setup

2.2.1 Simulation parameters

The simulations were done in COMSOL 5.5 using the Structural Mechanics component of the Acoustics module. The simulations used Finite Element Methods with quadratic elements, and with at least six mesh elements per wavelength. The material of the horn is assumed to be structural steel (the exact material was not given by the manufacturer), and the material properties used were the default properties in COMSOL. The highest frequency studied was 62 kHz, and the maximum element size was 0.0148 m. The study settings include geometric nonlinearities, and the modal search was done for 42 modes, which covered modes up to a little more than 60 kHz. The rest of the settings were the default settings in COMSOL.

The 3D model of the horn was provided by the Welding and Joining Institute, RWTH Aachen, and is shown in Figure 2. The length of the horn is along the x direction, the direction of vibration of the horn during welding. The z direction is the vertical direction, in which the horn applies the constant force against the workpieces and anvil. The horn has a length of 14.83 cm. The welding area, shown in green in Figure 2 (b), has knurls which dig into the upper workpiece. The knurls have 0.8 mm base side, 300 μm height and 90° apex angle.

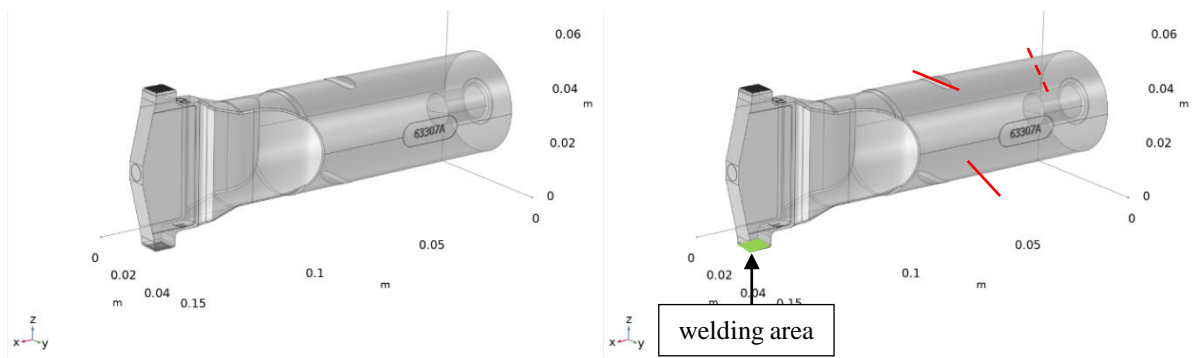


Figure 2: CAD model of horn (a) without the bolts and (b) with the bolts, shown as red lines. Dashed lines mean that the bolt goes through the horn, and full lines mean that the bolt is outside the horn. At the welding tip, the welding area, in green, is the area in contact with the upper worksheet.

2.2.2 Excitation and boundary conditions

Before the boundary conditions applied on the model are explained, the forces which act on the horn during welding and the expected modal behaviour of the horn should be described.

At $x=0$ m, shown on Figure 2, the horn is connected to the booster via a two-ended bolt, which runs through both of them. During welding, the vibrations of the booster are transmitted to the horn via this bolt and contact

between the horn and booster surfaces. The forces applied on the horn at $x=0$ m are a constant vertical force along the negative z axis, and a sinusoidal excitation force along the x axis: the welding excitation force. These forces are distributed along the bolt threads. Furthermore, a few centimetres forward along the x axis, another, smaller bolt runs radially through the horn from its outside perimeter makes contact with the two-ended bolt. This radial bolt is used to strengthen the connection between the booster and the horn. Therefore, the horn has an antinode of 20 kHz at $x=0$ m by design.

At $x=0.1483$ m, where the horn is in contact with the upper worksheet, there is another antinode of 20 kHz. Indeed, the wavelength of the longitudinal wave in the horn at 20 kHz is $5900 \frac{\text{m}}{\text{s}} / 20 \text{ kHz} = 0.295$ m, where 5900 is the speed of sound of the longitudinal wave in structural steel; this is double the horn length. Therefore, there is half a wavelength of 20 kHz in the horn, with two antinodes of opposite phase: one at $x=0$, and the other at $x=0.1483$ m. It is therefore expected for the horn to have a compression-elongation behaviour at 20 kHz. Furthermore, at $x=0.1483$ m, the forces applied on the horn are a vertical force in the positive z direction, the reaction to the force applied by the horn on the workpiece, and a friction force which resists the movements of the horn. In addition, it is expected that, at the welding tip, the horn amplifies frequencies received at $x=0$ m. Frequencies received from the transducer would then be amplified at the welding tip, leading to a more efficient welding.

Between the two antinodes, at $x=0.075$ m, is a node of the 20 kHz wave, with minimal vibrations. At the position of the node is a curved slit on the upper side of the horn. In this curved slit, perpendicular to the length of the horn, is placed a bolt. Via this bolt, the USMW machine applies a vertical force on the horn in the negative z direction. Furthermore, due to its threads and its position at the bottom of a curve, the bolt also applies a frictional resistance to vibrations along the welding direction. Since this bolt is placed at a node of the 20 kHz wave, it does not affect its propagation much, but dampens the vibrations at other frequencies, such as 40 kHz for example, which would have an antinode at that position. Furthermore, at this position, there is also another bolt, which touches the perimeter of the horn. This bolt is merely placed on the horn, not tightened against it. This bolt would not cause resistance against movement in the welding direction, but would resist any radial motion that pushes against it, for example in bending modes.

In this study, only the contact with the bolt in the curve was modeled using a fixed boundary condition. No other boundary conditions were applied on the horn.

3 Results

3.1 Measurement results

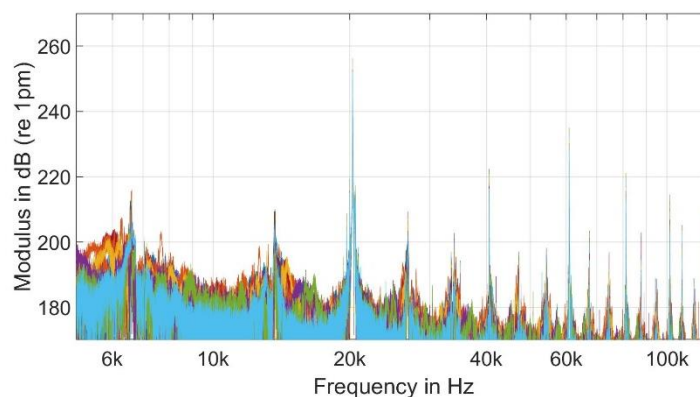


Figure 3: Frequency plot of horn vibrations

Figure 3 shows the frequency plot of 27 measurements of the horn vibrations. The different colours in the plot represent the different measurements. Since information on a specific measurement is not relevant for this analysis, a legend was not added to the plot for better readability. Furthermore, since the peaks have a certain width, have sometimes many smaller peaks close to them, and there are slight differences (less than 50 Hz) between different measurements, the frequencies with the highest amplitudes were chosen.

From Figure 3, it is clear that the peaks of all 27 measurements overlap very well. The welding frequency and its first two harmonics are visible at 20.28 kHz, 40.56 kHz and 60.85 kHz. Other frequencies are visible as well, and seem to be harmonics of a fundamental frequency 6.62 kHz. The harmonic series is given by

$$F_{The} = 6.62 \text{ kHz} * n \quad (1)$$

where $n=1, 2, \dots$

Table 1 lists the peak frequencies of Figure 3 in the row F_{Meas} , the theoretical harmonics in row F_{The} , and the difference between them. The difference between the theoretical frequencies and the measured frequencies is given in the row *Difference* and calculated by:

$$Difference(\%) = \frac{|F_{The} - F_{Meas}|}{F_{The}} * 100\% \quad (2)$$

where F_{The} is the theoretical frequency and F_{Meas} is the measured frequency.

Table 1: Peak frequencies from measurements, theoretical harmonics, and their differences

multiple	1	2	3	4	5	6	7	8	9
F_{The} (kHz)	6.62	13.24	19.86	26.48	33.1	39.72	46.34	52.96	59.58
F_{Meas} (kHz)	6.62	13.68	20.28	26.89	33.97	40.56	47.18	54.29	60.85
Difference (kHz)	0	0.44	0.42	0.41	0.87	0.84	0.84	1.33	1.27
Difference (%)	0.00	3.32	2.11	1.55	2.63	2.11	1.81	2.51	2.13
multiple	10	11	12	13	14	15	16	17	18
F_{The} (kHz)	66.2	72.82	79.44	86.06	92.68	99.3	105.92	112.54	119.16
F_{Meas} (kHz)	67.45	74.55	81.13	87.76	94.31	101.4	108.0	114.6	121.7
Difference (kHz)	1.25	1.73	1.69	1.7	1.63	2.1	2.08	2.06	2.54
Difference (%)	1.89	2.38	2.13	1.98	1.76	2.11	1.96	1.83	2.13

From Table 1, the measurement frequencies seem to fit the theoretical harmonic series quite well, with differences of less than 4% for all frequencies. The 20.28 kHz frequency has the highest amplitude, and contributes the most to the movement of the horn tip in the welding direction. Compared to the welding frequency, all other frequencies have much smaller amplitudes. The next frequencies with the largest amplitudes are 60.85, 40.56 and 81.13 kHz, with amplitudes larger than 0.1 μm , all harmonics of the welding frequencies, while the other ones have amplitudes. The other frequencies all have amplitudes ranging between 0.004 μm and 0.089 μm . The latter is reached by the 6.62 kHz frequency, the fundamental of the harmonic series.

Table 2 lists the displacement level L_{Disp} in dB re 1 pm of the measured displacement of the horn in the welding direction, in the x-direction, for each peak frequency. $x_{meas,peak}$ shows the amplitude of the displacement at each measurement frequency in the x direction, calculated from L_{Disp} . The amplitude of vibration of the horn changes during welding, so $x_{meas,peak}$ only shows a peak amplitude averaged over the entire welding. Example figures can be seen in [3]. $x_{meas,peak}$ for any frequency f is calculated by:

$$x_{meas,peak}(f) = \sqrt{10^{L_{Disp}(f)/10} * (1e - 12)^2 * 2} \quad (3)$$

From Table 2, it is clear that the 20.28 kHz frequency has the highest amplitude, and contributes the most to the movement of the horn tip in the welding direction. Compared to the welding frequency, all other frequencies have much smaller amplitudes. The next frequencies with the largest amplitudes are 60.85, 40.56 and 81.13 kHz, with amplitudes larger than 0.1 μm , all harmonics of the welding frequencies, while the other ones have amplitudes. The other frequencies all have amplitudes ranging between 0.004 μm and 0.089 μm . The latter is reached by the 6.62 kHz frequency, the fundamental of the harmonic series.

Table 2: Amplitude of the displacement of the peak frequencies

F_{Meas} (kHz)	6.62	13.68	20.28	26.89	33.97	40.56	47.18	54.29	60.85
L_{Disp} (dB re 1 pm)	216	210	256	209	202	222	197	198	235
$x_{meas,peak}$ (μm)	0.089	0.045	8.923	0.040	0.018	0.178	0.010	0.011	0.795
F_{Meas} (kHz)	67.45	74.55	81.13	87.76	94.31	101.4	108.0	114.6	121.7
L_{Disp} (dB re 1 pm)	203	196	221	202	189	214	205	189	210
$x_{meas,peak}$ (μm)	0.020	0.009	0.159	0.018	0.004	0.071	0.025	0.004	0.045

3.2 Simulation results

In total, 42 modes were calculated. Of those 42 modes, only a select few are presented here. The eigenmodes presented in this paper are the ones, which correspond best to the movement of the horn during welding, and which could be measured by the laser vibrometer, so which involved the vibration of the welding tip chiefly in the x direction, rather than in the y- or z -directions. The choice of which eigenmodes to show in this paper and which to discard was done manually by the authors, and was based on their knowledge of USMW to estimate the plausibility of occurrence of a specific modal behaviour during welding. For this estimate, two elements were taken into account: the closeness of a simulation eigenfrequency to a measured frequency, and the expected effect of the other boundary conditions, not included in the simulations but described in section 2.2.2. In other words, eigenmodes such as, for example, bending modes in the y-direction, torsional modes and modes which did not move the welding tip, or modes which are improbable because of the boundary conditions not included in the simulations and described in section 2.2.2, were discarded.

The eigenfrequencies are listed in section in section 3.2.1, and the eigenmodes are shown in section 3.2.2.

3.2.1 Eigenfrequencies

Table 3 lists the eigenfrequencies F_{Sim} of the relevant modes. The difference in percentage is calculated as

$$Difference = \frac{|F_{Sim} - F_{Meas}|}{F_{Meas}} * 100\% \quad (4)$$

Table 3: Comparison of measurement frequencies with simulation eigenfrequencies

F_{Meas} (kHz)	6.62	13.68	20.28	26.89	33.97	40.56	47.18	54.29	60.85
F_{Sim} (kHz)	NA	12.67	19.53	26.61	33.82	NA	49.44	54.36	61.69
Difference (kHz)	NA	1.01	0.75	0.28	0.15	NA	2.26	0.07	0.84
Difference (%)	NA	7.38	3.70	1.04	0.44	NA	4.79	0.13	1.38

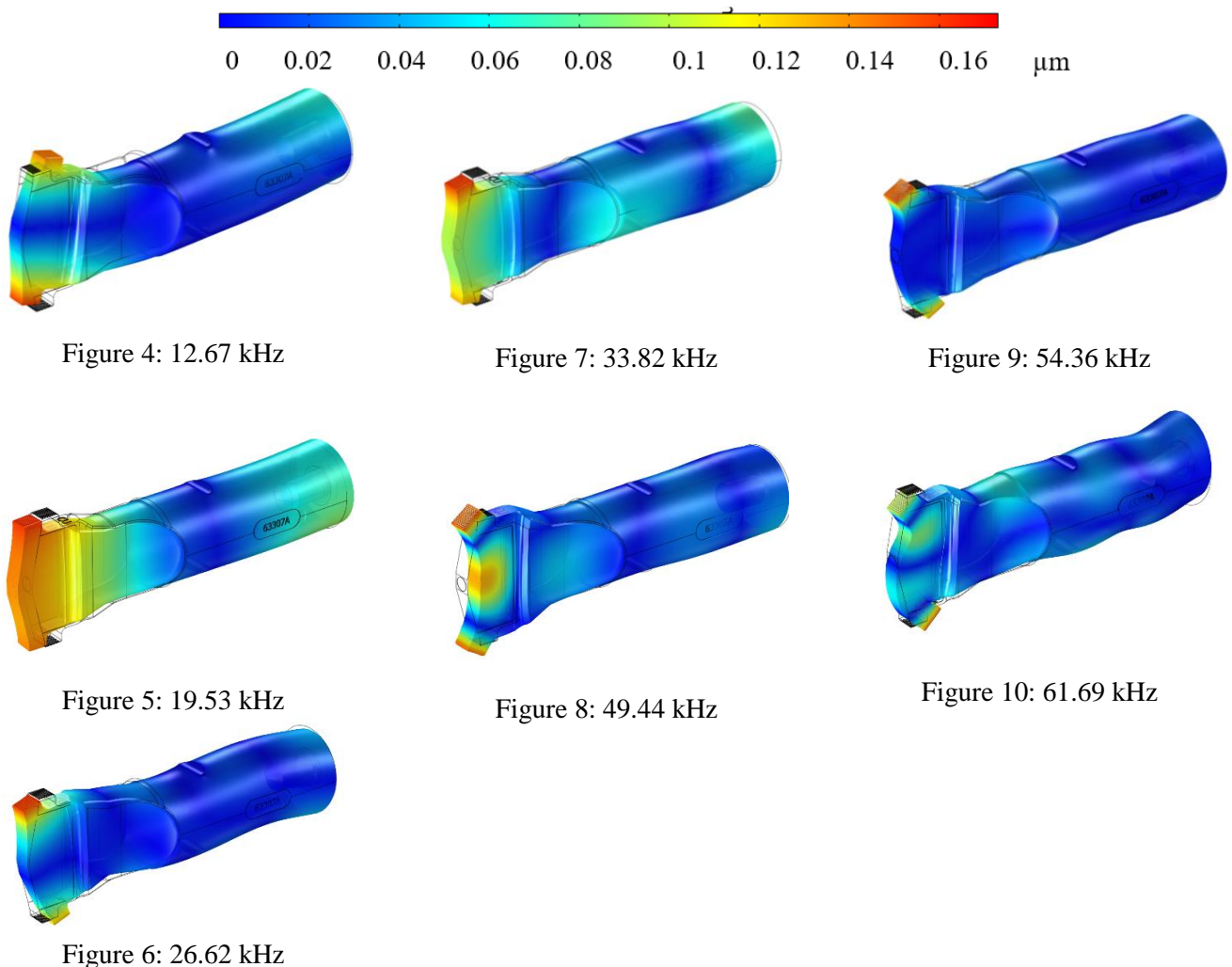
From Table 3, most of the measurement frequencies had corresponding eigenmodes, including the welding frequency, with some differences in frequencies. For most of the measured frequencies, the difference between simulated and measured frequency was less than 5%, except for the 13.68 kHz frequency with a difference of 7.38%. Based on the difference in kHz, though, the difference is less than 1 kHz for all frequencies except for

the measurement 13.68 kHz and 47.18 kHz. For frequencies less than the first harmonic of the welding frequency, 40 kHz, the simulation eigenfrequencies are smaller than the measured frequencies. For frequencies above 40 kHz, the eigenfrequencies are higher than the measured frequencies.

No suitable eigenmodes were found for the 6.62 kHz and 40.56 kHz measurement frequencies. The letters NA, standing for Not Applicable, were used to fill their respective columns.

3.2.2 Eigenmodes

Figures 4 to 10 show the eigenmodes of the frequencies. The colour map shows the absolute value of the displacement in the x direction over the entire modal cycle of displacement: red denotes large movements in the x direction, and blue denotes small movements. The wireframe in the plots shows the rest position of the horn. Note that the displacements shown in the figures were amplified 100 times for better visibility.



Starting with the 19.53 kHz eigenmode, the closest to the welding frequency, shown in Figure 5: this mode is a translational mode along the welding direction with almost no movement in the z direction, an antinode at the connection with the booster, another antinode at the welding tip, and a node around the middle of the horn, at the curved slit. Furthermore, the amplitude of the displacement at the welding tip, $0.16 \mu\text{m}$, is double the displacement at the back, $0.08 \mu\text{m}$. These elements were expected and described in section 2.2.2.

Looking at the other modes, all of them show amplification of the vibration amplitude from the excitation point of the horn, always in a shade of blue, to the welding tip, always in red. Similar to the 19.53 kHz eigenmode, they all show differences between their eigenfrequencies and the measurement frequencies. Furthermore, all of them also show noticeable displacement in the z direction, in addition to a displacement in the x-direction. These displacement are shown in more detail in Table 4.

To look at the displacement of the welding area of the horn in the x and z directions, x_{sim} and z_{sim} , a point was taken in the center of the welding area of the horn, the area in contact with the upper worksheet. x_{sim} and z_{sim} therefore show the movement of this point in the welding direction and normal to the workpiece when an eigenmode is excited. The ratio between them is given by z_{sim}/x_{sim} . The last row of the table shows the expected displacement of the welding area along the z-direction during welding, $z_{expected}$, calculated as:

$$z_{expected} = x_{meas,peak} * \frac{z_{sim}}{x_{sim}} \quad (5)$$

$z_{expected}$ is, of course, not representative of what actually happens during the actual welding. It allows us to compare the amplitude of displacement in the z-direction of our simulated eigenmodes while accounting for the difference in amplitude of the welding frequencies.

Table 4: Displacement along welding direction (x axis) and into the worksheets (z axis) of each eigenmode

Simulation (kHz)	NA	12.67	19.53	26.61	33.82	NA	49.44	54.36	61.69
x_{sim} (μm)	NA	0.162	0.143	0.133	0.134	NA	0.155	0.138	0.160
z_{sim} (μm)	NA	0.098	0.006	0.038	0.043	NA	0.046	0.014	0.013
z_{sim}/x_{sim}	NA	0.602	0.042	0.286	0.326	NA	0.296	0.100	0.081
$x_{meas,peak}$ (μm)	0.089	0.045	8.923	0.040	0.018	0.178	0.010	0.011	0.795
$z_{expected}$ (μm)	NA	0.027	0.375	0.011	0.006	NA	0.003	0.001	0.065

From Table 4, the highest $z_{expected}$ is 0.375 μm at 19.53 kHz, the welding frequency, although its z_{sim}/x_{sim} coefficient is the smallest. The second highest $z_{expected}$ comes from the second harmonic, 61.69 kHz, with a displacement of 0.065 μm , followed by 12.67 kHz with a displacement of 0.027 μm and 26.61 kHz with 0.011 μm . The other frequencies have displacements of less than 0.01 μm .

4 Discussion

From Figure 3, the overlap of the frequencies in all measurements shows that the measurement is repeatable, and these frequencies should be expected in other welding situations if the same horn geometry as the one studied in this paper is used. Looking at the measurement results in Table 3, since the peaks found in the measurements fit a harmonic series so well, it is highly likely that these harmonics come from the transducer itself, rather than be generated by other elements in the transmission chain from transducer to horn. These frequencies could be a by-product of generating the welding frequency. It is possible that the friction on the horn during welding puts extra strain on the transducer, driving it into a non-linear regime in which the frequencies other than the welding frequency are more pronounced. Such excitation, small at the output of the transducer, would then excite modes of the horn and be amplified at the welding tip.

In the simulations, the eigenmode found at 19.53 kHz fits the description of the horn vibration during welding well: the movement pattern it displays corresponds well to the expected behaviour of the horn during welding. This is a first indication that the simulations were set up correctly. Such a translational displacement with very little variations in the z direction, combined with a normal force into the workpiece, would create controllable, repeatable friction between the horn and the upper worksheet. The difference between the measured and welding frequency is small, and can be seen as a natural occurrence of the simulation limitations.

The differences between the simulation eigenfrequencies and the measurement frequencies could be due to multiple factors: differences in the material properties between the horn model and the real horn, not adding all boundary conditions, and the non-ideal modelling of boundary conditions. These points are all limitations of the simulations done here. Nevertheless, a good agreement was reached in some cases: the modal behaviour of the welding frequency is as expected in real measurements, and the difference in calculated frequency was small. All calculated eigenfrequencies are similar to the measured eigenfrequencies, with differences of less than 10%, and often less than 5%. There is therefore good agreement between the modal analysis and the experimental measurements.

No eigenmode was found to fit the 40 kHz measurement frequency. This makes sense, because such a mode would have an antinode at the curved slit, where a fixed boundary condition is applied during welding. As for the 6.62 kHz measurement frequency, no corresponding eigenmode was found. This could be due to the differences between the simulation setup and the forces which are applied on the horn during actual welding. It is possible that one such mode could be found if more boundary conditions are applied in the simulation.

Looking at the changes in the z direction, it is clear that the highest displacement comes from the welding frequency. Even combining the displacement of all frequencies coherently, the total average displacement would still be less than 1 μm . This is three orders of magnitude less than the depth of the horn knurl, 300 μm , and the penetration of the horn into the workpiece. It is safe to assume that the horn is always in contact with the workpiece, and that the horizontal excitation of the workpiece is always happening. However, this does not give us an indication of whether the vertical force applied by the horn on the workpiece fluctuates at any of the frequencies excited. This might also be frequency-dependent, since vertical displacements of similar amplitudes are found for frequencies both noticeably higher and lower than the welding frequency.

From the results of this study can be suggested a hypothesis to explain the frequency content of the measurement results: during welding, the transducer generates a harmonic series with a fundamental frequency at 6.62 kHz, and in which its second harmonic, the welding frequency, has a much higher amplitude than all other frequencies in the series. The frequencies in this harmonic series then excite corresponding modes in the horn, which lead to non-zero vibrations of the welding tip at those frequencies. In the x direction, the welding tip would then vibrate not only at the welding frequency, but also at the frequencies excited by the harmonic series. Furthermore, the eigenmodes excited would lead to vibrations of the welding tip along the z direction, into and away from the workpiece. These extra displacements of the welding tip in both x and z directions might have an effect on the friction between the horn and the upper worksheet: vibrations in the x direction would affect the relative movement between the horn and upper workpiece, and vibrations in the z direction might affect the normal force applied by the horn on the workpiece, both of which are primary parameters of friction.

It is not clear at the moment whether such movements actually have any effect on the welding process, as the transfer of forces from the horn through the workpieces to the anvil is complicated. According to [1], friction is an important element of USMW not only between the worksheets, but also at the interface between the upper worksheet and the horn, and at the interface between the lower worksheet and the anvil. The friction in these friction sites depends not only on the normal force applied by the horn on the upper worksheet and the relative movement between them, but also on how they transfer to the upper worksheet-lower worksheet and lower worksheet-anvil interfaces. To investigate the effect of these x- and z-movements on friction generation, many further elements would have to be taken into consideration: the period of the x- or z-displacement relative to a welding frequency cycle, relative to the period of elastic relaxation of the upper sheet, or the amplitude of z-displacement relative to the horn penetration into the upper worksheet, to name a few. This could lead to interesting effects: for example, if the changes in the z direction are much faster than a welding period, this could lead to a hammering effect similar to a jack hammer, and the x-displacement would resemble more closely stick-slip behaviour.

Should one want to avoid such modal behaviour of the horn, it might be possible by adding boundary conditions to the horn, or altering the horn geometry adequately. Care should then be taken to avoid exciting modes of the new horn, or at least those which might lead to unwanted behaviour. Furthermore, it is also possible that other modes of the horn not measured in these experiments are present, for example in the y direction. This is improbable, due to the direction of excitation of the transducer into the horn, but not impossible. Measurements of the horn surface perpendicular to the welding direction would be a good and fast way to check whether such movements occur. Finally, it is good to remember that the comparison between simulations and measurements was limited to a maximum frequency of about 65 kHz. Movement of the welding tip of the horn has been measured in frequencies up to 120 kHz, and the modal behaviour of the horn at those frequencies might affect the welding process as well.

5 Conclusion

Fluctuations of weld strength happen during USMW. Measurements have shown that the vibrations of the welding tip of the horn during welding contain not just the welding frequency, but other frequencies as well. These frequencies were found to be part of a harmonic series, of which the welding frequency is the second harmonic, and most likely originating from the transducer of the USMW machine during welding. The harmonics of this series matched some eigenmodes of the USMW horn studied. From the modal analysis, the displacements of the welding tip of the horn into the workpiece during welding was estimated. Further work is required to estimate whether these displacements actually have an effect on the weld strength.

Acknowledgements

This work was supported by DFG in the grant VO600/43-1.

The main author would like to thank his colleagues from the Technical Acoustics group at the Institute of Hearing Technology and Acoustics for their help in setting up the simulations, namely S. Kersten, P. Schäfer, C. Dreier and M. Berzborn, as well as his other colleagues from the TA group for their help in thinking about the results. Thanks also go to F. Müller from the Welding and Joining Institute, RWTH Aachen, for providing the CAD model of the horn and describing the forces applied on the horn.

References

- [1] Balz, I.: Prozessanalyse der thermo-mechanischen Vorgänge während der Verbindungsbildung beim Metall-Ultraschallschweißen. Doctoral Dissertation RWTH Aachen University. Aachener Berichte Fügetechnik, Band 3/2020, ISBN 978-3-8440-7537-3, pp. 1-149, 2020.
- [2] de Vries, E.: Mechanics and Mechanisms of Ultrasonic Metal Welding. Doctoral dissertation, Ohio State University. ISBN 978-0-4966-9934-6, pp. 1-253, 2004.
- [3] Abi Raad, E.; Balz, I.; Reisgen, U.; Vorländer, M. Derivation of characteristic vibroacoustic parameters in Ultrasonic Sheet Metal Welding. Proc. *DAGA 2020*, Hannover, Germany, March 16-19, 2020, pp 1129-1132.
- [4] Schöneweiß, R.; Kling, C.; Koch, C. A laboratory study for occupational safety and health on the structure of airborne ultrasound fields. *Acta Acustica* 4 (4), 2020.
- [5] Balz, I.; Reisgen, U.; Schiebahn, A.; Abi Raad, E.; Vorländer, M.: Process monitoring of ultrasonic metal welding of battery tabs using external sensor data. Proc. *AJP 2019*. Ponta Delgada, Azores, October 24-25, 2019. pp 1-18.